ChemPubSoc Europe

DOI: 10.1002/chem.201404923

CHEMISTRY
A European Journal
Full Paper

Chalcogenometallates

Synthesis, Structural Characterization, and Physical Properties of $Cs_2Ga_2S_5$, and Redetermination of the Crystal Structure of Cs_2S_6

Daniel Friedrich, Florian Pielnhofer, Marc Schlosser, Richard Weihrich, and Arno Pfitzner*[a]

Dedicated to Professor Arndt Simon on the occasion of his 75th birthday

Abstract: The reaction of CsN_3 with GaS and S at elevated temperatures results in $Cs_2Ga_2S_5$. Its crystal structure was determined from single-crystal X-ray diffraction data. The colorless solid crystallizes in space group $C2/c$ (no. 15) with $V=1073.3(4)$ Å^3 and $Z=4$. $Cs_2Ga_2S_5$ is the first compound that features one-dimensional chains $^1_\infty[Ga_2S_3(S_2)^{2-}]$ of edge- and corner-sharing GaS_4 tetrahedra. The vibrational band of the S_2^{2-} units at 493 cm^{-1} was revealed by Raman spectroscopy. $Cs_2Ga_2S_5$ has a wide bandgap of about 3.26 eV. The thermal decomposition of CsN_3 yields elemental Cs, which reacts with sulfur to provide Cs_2S_6 as an intermediate product. The crystal structure of Cs_2S_6 was redetermined from selected single crystals. The red compound crystallizes in space group $P\bar{1}$ with $V=488.99(8)$ Å^3 and $Z=2$. Cs_2S_6 consists of S_6^{2-} polysulfide chains and two Cs positions with coordination numbers of 10 and 11, respectively. Results of DFT calculations on $Cs_2Ga_2S_5$ are in good agreement with the experimental crystal structure and Raman data. The analysis of the chemical bonding behavior revealed completely ionic bonds for Cs, whereas Ga–S and S–S form polarized and fully covalent bonds, respectively. HOMO and LUMO are centered at the S_2 units.

Introduction

A large variety of chalcogenometallates of group 13 metals containing alkali metal cations have already been investigated.[1] Such semiconductors are known, for example, for their nonlinear optical properties and their use as IR detectors.[2,3] Most of the known compounds in the ternary systems of alkali metal, triel, and chalcogen consist of linked MQ_4 (M = Al, Ga, In; Q = S, Se, Te) tetrahedra embedded in a cationic surrounding. These linked tetrahedra form anionic units ranging from discrete tetrahedra to more complex one-, two-, or three-dimensional polyanionic networks. Among the three known phases in the ternary system cesium, gallium, and sulfur, the crystal structures of $CsGaS_2$[4] and $CsGaS_3$[5] contain infinite one-dimensional thiogallate anions. $CsGa_3S_5$[6] exhibits a two-dimensional layered structure. Hitherto, $CsGaS_3$ was the only compound among group 13 chalcogenometallates with alkali metal counterions that contains polysulfide units.

Recently, we reported the discovery of $Cs_2Ga_2S_5$,[7] a new member of the group of polysulfide-based thiogallates. Herein, we describe the structural characterization, some physical properties, and theoretical investigations of this new material. The anionic structure of the title compound is closely related to the anionic chains $^1_\infty[M_2Se_3(Se_2)^{2-}]$ (M = Ga, In) found in $Cs_2Ga_2Se_5$[8] and related compounds containing organic cations.[9–13] However, $Cs_2Ga_2S_5$, is the first example featuring the thiogallate chain $^1_\infty[Ga_2S_3(S_2)^{2-}]$. The simultaneous appearance of disulfide $[S_2]^{2-}$ and sulfide $[S]^{2-}$ ions therein provokes the question of the nature of the bonds to Ga and within the SS entities.

We also report on the redetermination of the crystal structure of Cs_2S_6, which was obtained as a side product during the synthesis of $Cs_2Ga_2S_5$. There is some confusion in the literature concerning this compound,[14,15] and the availability of precise structural data seems highly desirable.

Results and Discussion

The crystal structure of $Cs_2Ga_2S_5$

$Cs_2Ga_2S_5$ forms air- and moisture-stable, colorless crystals. The solid crystallizes in the monoclinic space group $C2/c$ (no. 15) with $a=12.5885(7)$, $b=7.1429(4)$, $c=12.3441(7)$ Å, $\beta=108.338(5)^\circ$, $V=1053.6(1)$ Å^3 ($T=123$ K, single-crystal data); $a=12.688(2)$, $b=7.191(1)$, $c=12.389(2)$ Å, $\beta=108.28(1)^\circ$, $V=1073.3(4)$ Å^3 ($T=293$ K, powder data); and $Z=4$.

An additional sulfur site S33 was introduced for the only residual electron-density maximum in the center of the disulfide dumbbell S3–S3. These two sites were refined by using a constraint for the occupation factors to ensure charge balance. The final structure model contained 85.8% S_2^{2-} and 14.2% S^{2-} ions at this position (Figure 1). On taking this disorder into account, the R values dropped to $R_1=0.0456$ and $wR_2=0.0751$ (for all data). Several crystals were investigated, and all showed

[a] D. Friedrich, F. Pielnhofer, M. Schlosser, R. Weihrich, Prof. Dr. A. Pfitzner
Institut für Anorganische Chemie, Universität Regensburg
Universitätsstrasse 31, 93040 Regensburg (Germany)
E-mail: arno.pfitzner@chemie.uni-regensburg.de

Supporting information for this article is available on the WWW under http://dx.doi.org/10.1002/chem.201404923.

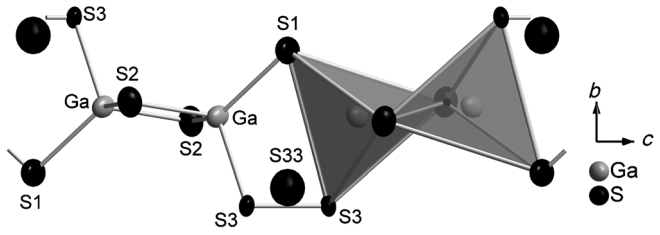

Figure 1. Segment of the anionic chain $^{1}_{\infty}[Ga_2S_3(S_2)^{2-}]$, showing the local coordination of Ga with respect to the disorder present in the S_2^{2-} unit (ellipsoids represent 90% probability). Occupancies are 85.8% for S3 and 14.2% for S33.

this kind of disorder of S_2^{2-} and S^{2-} at this position. Similar observations were made for $Cs_2Ga_2Se_5$[8] and other polychalcogenide-containing compounds,[16,17] that is, this disorder seems to be an intrinsic phenomenon for these compounds.[8] No formation of solid solutions was observed for these compounds within the investigated regions.

Details of the structure solution and refinement and the final crystallographic data for $Cs_2Ga_2S_5$ are listed in Table 1. The atomic coordinates and displacement parameters are summarized in Table 2, and the interatomic distances in Table 3.

Table 1. Crystallographic data, details of data collection, and crystal structure refinement of $Cs_2Ga_2S_5$ and Cs_2S_6.[a]

	$Cs_2Ga_2S_5$	Cs_2S_6
formula weight	565.5	458.2
color/shape	colorless/rod	red/needle
crystal system, space group	monoclinic, *C*2/*c*	triclinic, $P\bar{1}$
a[b] [Å]	12.5885(7)	4.658(1)
b[b] [Å]	7.1429(4)	9.174(1)
c[b] [Å]	12.3441(7)	11.537(1)
α[b] [°]	90.0	84.842(8)
β[b] [°]	108.338(5)	84.810(7)
γ[b] [°]	90.0	89.240(8)
V [Å^3]	1053.6(1)	488.99(8)
Z	4	2
ρ_{calcd} [g cm^{-3}]	3.5642	3.1108
T [K]	123	293
λ [Å]	0.71073	
$\mu(Mo_{K\alpha})$ [mm^{-1}]	12.827	8.643
θ [°]	3.32–29.12	2.97–26.62
index range	$-16 \le h \le 16$	$-5 \le h \le 5$
	$-9 \le k \le 9$	$-10 \le k \le 10$
	$-16 \le l \le 16$	$-14 \le l \le 14$
collected reflns	5529	5008
independent reflns	1271	1727
R_{int}	0.0539	0.0438
completeness to $\theta = 25°$	99.9%	94.8%
extinction coefficient G_{iso}	–	0.146(5)
no. of refined parameters	48	74
no. of constraints	1	0
GoF	1.29	1.21
R_1, wR_2 [$I > 3\sigma(I)$]	0.0317, 0.0694	0.0278, 0.0612
R_1, wR_2 (all data)	0.0456, 0.0751	0.0326, 0.0647
largest diff. peak & hole [e Å^{-3}]	1.00, −1.08	0.63, −0.50

[a] Further details on the crystal structure investigations may be obtained from the Fachinformationszentrum Karlsruhe, 76344 Eggenstein-Leopoldshafen, Germany (fax: (+49) 7247-808-666; E-mail: crysdata@fiz-karlsruhe.de), on quoting the depository number CSD-428611 ($Cs_2Ga_2S_5$) and CSD-428612 (Cs_2S_6). [b] Lattice constants from single crystals.

Table 2. Atomic coordinates and equivalent isotropic displacement parameters U_{eq} [Å^2] for $Cs_2Ga_2S_5$.

Atom	Wyckoff position	SOF	*x*	*y*	*z*	U_{eq}[a]
Cs	8f	1	0.1843(1)	0.4806(1)	0.1339(1)	0.0150(1)
Ga	8f	1	0.4867(1)	0.4840(1)	0.1125(1)	0.0106(2)
S1	8f	1	1/2	0.6968(4)	1/4	0.0186(8)
S2	4e	1	0.3548(1)	0.5311(3)	−0.0602(1)	0.0144(5)
S3	8f	0.858(7)	0.4390(1)	0.1973(3)	0.1698(1)	0.0090(6)
S33	4e	0.142[b]	1/2	0.255(3)	1/4	0.029(8)[c]

[a] U_{eq} is defined as one third of the trace of the orthogonalized U_{ij} tensor. [b] The site occupancy factors (SOF) for S3 and S33 were constrained, and therefore no estimated standard deviation (e.s.d) was calculated for SOF(S33). [c] The displacement parameters for position S33 are quite high, and the e.s.d. is also high due to the very low occupancy, as already observed for $Cs_2Ga_2Se_5$.[6]

Table 3. Selected bond lengths and angles for $Cs_2Ga_2S_5$.

Bond lengths [Å]				Bond angles [°]	
Ga–S1	2.277(2)	Cs–S1	3.704(2)	S1-Ga-S1^{viii}	100.77(6)
Ga–S1^{viii}	2.284(2)	Cs–S1^{ii}	3.761(2)	S1-Ga-S2	117.81(7)
Ga–S2	2.245(2)	Cs–S1^{iii}	3.599(2)	S1-Ga-S3	103.57(6)
Ga–S3	2.307(2)	Cs–S1^{vii}	3.711(2)	S3-Ga-S1^{viii}	112.33(7)
Ga–S33	2.33(2)	Cs–S2	4.081(1)	S3-Ga-S2	109.46(7)
		Cs–S2^{iv}	3.693(2)	S2-Ga-S1^{viii}	112.44(5)
S3–S3^{vi}	2.089(2)	Cs–S3	3.698(2)	Ga-S1-Ga^{viii}	79.23(5)
Ga–Ga^{viii}	2.908(1)	Cs–S3^{v}	3.604(2)		
Ga–Ga^{vi}	3.305(1)	Cs–S3^{i}	3.610(2)		
		Cs–S3^{ix}	3.798(2)		
		Cs–S33^{v}	3.66(1)		

[a] Symmetry codes used to generate equivalent atoms: i) $-x+0.5$, $y+0.5$, $-z+0.5$; ii) $-x+0.5$, $-y+0.5$, $-z$; iii) $-x+0.5$, $-y+1.5$,$-z$; iv) $x-0.5$, $y-0.5$, z; v) $x-0.5$, $y+0.5$, z; vi) $-x+1$, y, $-z+0.5$; vii) x, $-y+1$, $z+0.5$; viii) $-x+1$, $-y+1$, $-z$, ix) $0.5-x$, $0.5-y$, $-z$.

The crystal structures of both $Cs_2Ga_2S_5$ and $Cs_2Ga_2Se_5$ have a similar chalcogenometallate chain as the most important feature. However, they are quite different and not isotypic. Both compounds crystallize in the space group *C*2/*c* but with considerably different cell dimensions and atom positions. $Cs_2Ga_2S_5$ features infinite chains $^{1}_{\infty}[Ga_2S_3(S_2)^{2-}]$ parallel to [001], as shown in Figure 2. Cesium atoms separate these thiogallate polyanions. Trivalent gallium has a slightly distorted tetrahedral coordination environment formed by three S^{2-} ions and one S atom of the S_2^{2-} unit. The Ga–S bond lengths range from d(Ga–S) = 2.245(2) Å to d(Ga–S) = 2.307(3) Å with a mean bond length of $\bar{d}$(Ga–S) = 2.279 Å. Distances between the gallium atom and the disulfide ions are longer than those to the sulfide ions, as already observed in $CsGaQ_3$ (Q = S, Se)[5,21] and $Cs_2Ga_2Se_5$.[8] The S-Ga-S angles range from 100.77(6) to 117.81(7)°. The observed bond lengths and angles are in good agreement with those reported for similar compounds.[4–6] The bond length of the disulfide ion d(S3–S3) = 2.089(2) Å is also in good agreement with those of comparable compounds.[5,22]

Two GaS_4 tetrahedra are condensed through a common edge to form double tetrahedra Ga_2S_6. The Ga_2S_6 units are connected by one common corner and one disulfide dumbbell, re-

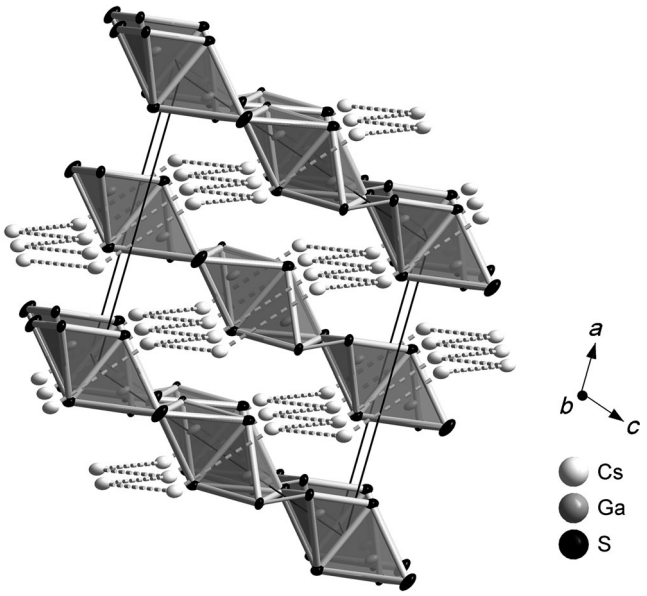

Figure 2. Section of the crystal structure of $Cs_2Ga_2S_5$ showing the $^1_\infty[Ga_2S_3(S_2)^{2-}]$ chains oriented along [001] (ellipsoids at 90% probability) embedded in the network of Cs ions. Fragmented lines indicate the topology of the cesium network.

sulting in an infinite one-dimensional anionic chain along [001]. This chain can alternatively be described as alternating five-membered $Ga_2S(S_2)$ rings and four-membered Ga_2S_2 rings linked by common corners. Two different distances d(Ga–Ga) = 2.908(1) Å and d(Ga–Ga) = 3.305(1) Å are observed for the alternating connection modes in the chain. The longer distance is present in the five-membered $Ga_2S(S_2)$ rings. Anionic chains $^1_\infty[Ga_2S_3(S_2)^{2-}]$ are related to the chains in $CsGaS_2$[4] and $CsGaS_3$.[5] The substitution of chalcogenide ions by dichalcogenide moieties and the resulting chains are depicted in Scheme 1. This is similar to the polychalcogenide flux reactions described, for example, by Kanatzidis et al.[23] This description of the structure applies for the majority part assuming fully occupied S3 positions. The position S33, however, is partially occupied for about 7% and thus S3 cannot be fully occupied. The coordination of Ga remains fourfold, but the coordination number of Cs is reduced due to this exchange within a sphere of 4.1 Å radius.

The recently reported compounds $Cs_2Ga_2Se_5$,[8] $[C_6H_{16}N_2][In_2Se_3(Se_2)]$,[9] $[M(C_{12}H_8N_2)_3][In_2Se_3(Se_2)]H_2O$ (M = Ni, Fe),[10] $[C_4H_{14}N_2][Ga_2Se_3(Se_2)]$,[11] $[C_6H_{16}N_2][Ga_2Se_3(Se_2)]$,[12] and $[Mn(C_2H_8N_2)_3][In_2Se_3(Se_2)]$[13] contain analogous chains $^1_\infty[M_2Se_3(Se_2)^{2-}]$. However, $Cs_2Ga_2S_5$ is the first representative featuring such an anionic thiometallate chain.

The cesium atoms are tenfold coordinated by sulfur atoms within a sphere of 4.1 Å radius in an irregular coordination polyhedron (Figure 3). The coordination polyhedra of the Cs

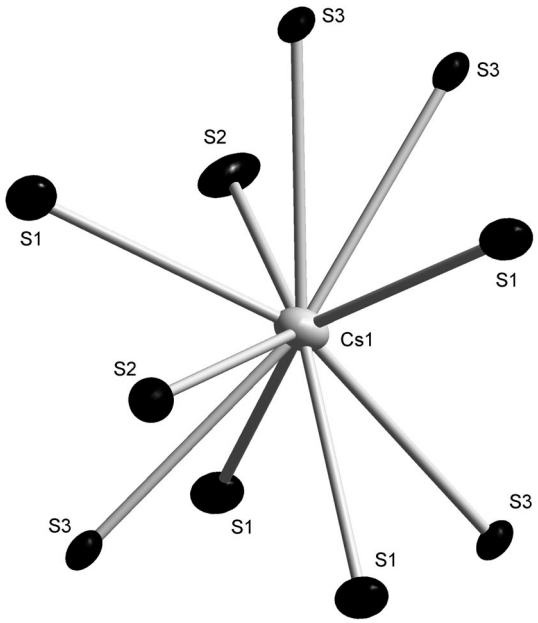

Figure 3. Local coordination of Cs in $Cs_2Ga_2S_5$ within a sphere of 4.1 Å radius (ellipsoids represent 90% probability).

ions share common edges and faces. The Cs–S bond lengths range from d(Cs–S) = 3.599(2) Å to d(Cs–S) = 4.081(1) Å with a mean bond length of d(Cs–S) = 3.726 Å. These values are in good agreement with those of comparable compounds.[4,5]

If distances of d(Cs–Cs) < 5 Å are taken into account, one observes puckered layers of Cs in $[10\bar{1}]$. The cesium atoms are arranged as six-membered rings in chair conformation therein. The anionic chains penetrate this network along [001] (Figure 2) and are arranged as a hexagonal rod packing.

Redetermination of the crystal structure of Cs_2S_6

$Cs_2Ga_2S_5$ seems to result from the formation of polysulfide ions during the reaction. Clearly a cesium polysulfide is formed prior to the final product. This polysulfide was identified as Cs_2S_6 by Raman spectroscopy. Because of contradictions regarding the crystal structure data for Cs_2S_6 in the literature[14,15] and to obtain state-of-the-art data we redetermined the crystal structure. Details of the structure solution, refinement, and the final crystallographic data for Cs_2S_6 are listed in Table 1. Atomic coordinates and displacement parameters are summarized in Table 4, and the interatomic distances in Table 5.

Dicesium hexasulfide crystallizes in the triclinic space group $P\bar{1}$ with a = 4.658(1), b = 9.174(1), c = 11.537(1) Å; α = 84.842(8), β = 84.810(7), γ = 89.240(8)°; V =

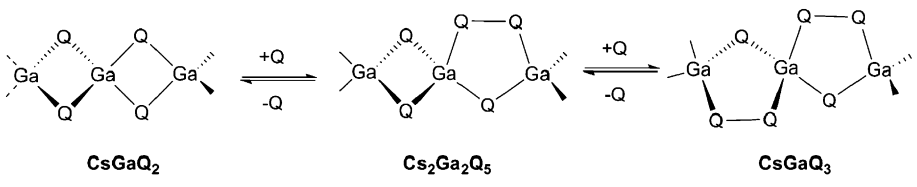

Scheme 1. Reaction scheme for the substitution of chalcogenide ions by dichalcogenide moieties and the resulting chains.

Table 4. Atomic coordinates and equivalent isotropic displacement parameters U_{eq} [Å^2] for Cs_2S_6.

Atom	Wyckoff position	x	y	z	U_{eq}[a]
Cs1	2i	0.9486(1)	0.6740(1)	0.0966(1)	0.0318(1)
Cs2	2i	0.8980(1)	0.3092(1)	0.3863(1)	0.0291(1)
S1	2i	0.0470(1)	0.3448(2)	0.1475(1)	0.0271(5)
S2	2i	0.4982(3)	0.1347(2)	0.1031(1)	0.0318(5)
S3	2i	0.2034(3)	0.0108(2)	0.2097(1)	0.0316(5)
S4	2i	0.3584(3)	0.9690(2)	0.3714(1)	0.0297(5)
S5	2i	0.6362(3)	0.7922(2)	0.3655(1)	0.0269(5)
S6	2i	0.4156(3)	0.6145(2)	0.3314(1)	0.0275(5)

[a] U_{eq} is defined as one-third of the trace of the orthogonalized U_{ij} tensor.

Table 5. Selected bond lengths and angles for Cs_2S_6.

Bond lengths [Å]				Bond angles [°]	
S1–S2	2.037(2)			S1-S2-S3	108.65(9)
S2–S3	2.043(2)			S2-S3-S4	108.68(9)
S3–S4	2.063(2)			S3-S4-S5	108.52(8)
S4–S5	2.064(2)			S4-S5-S6	109.03(9)
S5–S6	2.025(2)				
Cs1–S1	3.750(2)	Cs2–S1	3.537(2)		
Cs1–S1^{i}	3.886(2)	Cs2–S1^{i}	3.653(2)		
Cs1–S1^{ii}	3.739(2)	Cs2–S3^{i}	3.748(2)		
Cs1–S1^{iii}	3.582(2)	Cs2–S4^{iii}	3.735(2)		
Cs1–S2^{ii}	3.653(2)	Cs2–S4^{vii}	3.771(2)		
Cs1–S2^{iii}	3.573(2)	Cs2–S4^{viii}	4.059(1)		
Cs1–S3^{iv}	3.709(2)	Cs2–S5^{v}	3.680(2)		
Cs1–S5	3.515(2)	Cs2–S5^{vi}	3.789(2)		
Cs1–S6	3.625(2)	Cs2–S6	3.615(2)		
Cs1–S6^{i}	3.625(2)	Cs2–S6^{i}	3.694(2)		
		Cs2–S6^{v}	3.571(2)		

[a] Symmetry codes used to generate equivalent atoms: i) $x+1, y, z$; ii) $-x+2, -y+1, -z$; iii) $-x+1,-y+1,-z$; iv) $x+1,y+1,z$; v) $-x+1,-y+1,-z+1$; vi) $-x+2,-y+1,-z+1$; vii) $x+1$,y-1,z; viii) $-1+$x, y, z.

488.99(8) Å^3; $Z=2$ (293 K, single-crystal data) and $a=4.669(1)$, $b=9.211(1)$, $c=11.550(5)$ Å; $\alpha=84.69(2)$, $\beta=84.81(2)$, $\gamma=89.17(3)^\circ$; $V=492.5(4)$ Å^3 (293 K, powder data). The crystal structure was solved by charge-flipping methods with SUPERFLIP,[19] implemented in Jana2006,[20] and refined to $R_1=0.0326$ and $wR_2=0.0647$ (for all data) by full-matrix least squares methods with Jana2006.[20] Among alkali metal polysulfides only K_2S_6[24] and Cs_2S_6[14,15] are known to contain anionic chains S_6^{2-} embedded in a cationic alkali metal substructure. However, among group 11 chalcogenometallates, examples containing S_6^{2-} chains[25] and intergrown Cs_2S_6[26] have been reported by Kanatzidis et al. The crystal structures of monoclinic K_2S_6 and triclinic Cs_2S_6 are similar, but not identical. Cs_2S_6 contains long unbranched, nonplanar polychalcogenide chains (Figure 4). The terminal S–S bond lengths in the S_6^{2-} ion of d(S1–S2) = 2.037(2) Å and d(S5–S6) = 2.025(2) Å are significantly shorter than the central S–S bonds of d(S2–S3) = 2.043(2), d(S3–S4) = 2.063(2), and d(S4–S5) = 2.064(2) Å. The S-S-S angles are almost identical and range from 108.5(1) to 109.0(1)°, and dihedral angles in the chain are −76.5(1), −82.9(1), and −62.2(2)°. The two crystallographically independent cesium atoms are ten- and elevenfold coordinated by sulfur in irregular coordination polyhedra (Figure 4). The Cs–S distances range from d(Cs–S) = 3.515(2) to d(Cs–S) = 4.059(1) Å with no obvious trend of shorter distances for terminal or central sulfur atoms. The observed bond lengths and angles are in good agreement with those reported for comparable compounds.[25–30]

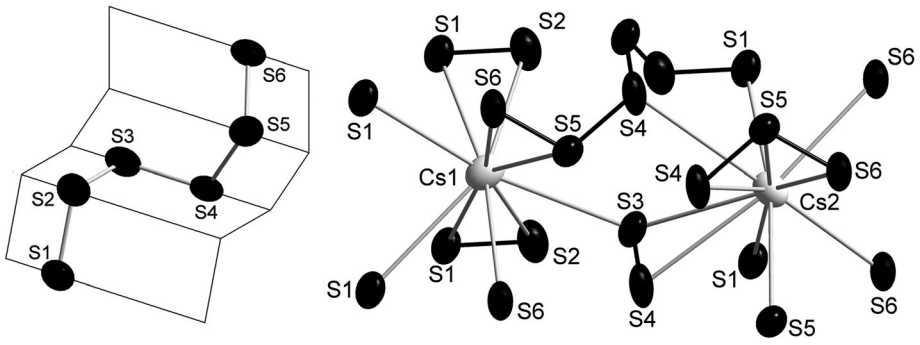

Figure 4. Left: Conformation of the hexasulfide ion S_6^{2-} in Cs_2S_6. (dihedral angles: S1-S2-S3-S4 −76.5(1), S2-S3-S4-S5 −82.9(1), and S3-S4-S5-S6 −62.2(2)°). Right: Local coordination of both Cs sites. Ellipsoids represent 90% probability.

Vibrational spectroscopy

The measured and simulated Raman spectra of $Cs_2Ga_2S_5$ are shown in Figure 5. The peak at 493 cm^{-1} (DFT: 459 cm^{-1}) can be assigned to S–S stretching vibrations.[5,31] Vibrational bands at 386 (377), 348 (341), 324 (313), and 291 (282) cm^{-1} (calculated wavenumbers in parentheses) most likely result from Ga–S stretching modes,[5,32] whereas the peaks at lower wavenumbers can all be assigned to Cs–S stretching modes or lattice vibrations.[5] Calculated Raman shifts are in good agreement with measured data (Table 6).

Optical properties

The bandgap of $Cs_2Ga_2S_5$ was determined by UV/Vis diffuse-reflectance spectroscopy (Figure 6). A modified Kubelka–Munk function[33] was used to calculate the absorption data. Extrapolation of the linear part to the baseline resulted in a wide bandgap of 3.26 eV (380 nm). The observed bandgap is slightly larger than that of the similar compound $CsGaS_3$ ($\approx$3 eV), and corresponds quite well with colorless crystals.

Electronic-structure calculations

Electronic-structure calculations for $Cs_2Ga_2S_5$ were performed in the DFT framework starting from a fully ordered crystal

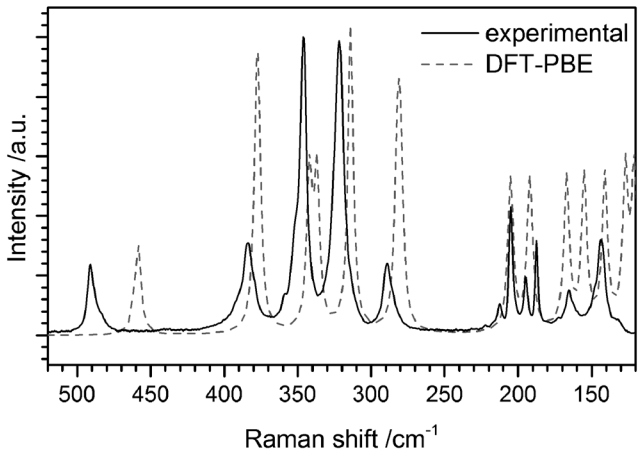

Figure 5. Measured (solid line) and calculated (dashed line) Raman spectrum of $Cs_2Ga_2S_5$.

Table 6. Measured and calculated (DFT) frequencies [cm^{-1}] of Raman shifts in $Cs_2Ga_2S_5$.

Exptl	DFT	Symmetry	DFT	Symmetry
493	459	A_g	280	A_g
386	378	B_g	205	A_g
	377	A_u	192	B_g
348	342	B_g	167	A_g
	337	A_g	155	B_g
324	314	A_g	141	B_g
	314	B_g	127	B_g
291	282	B_g	121	A_g

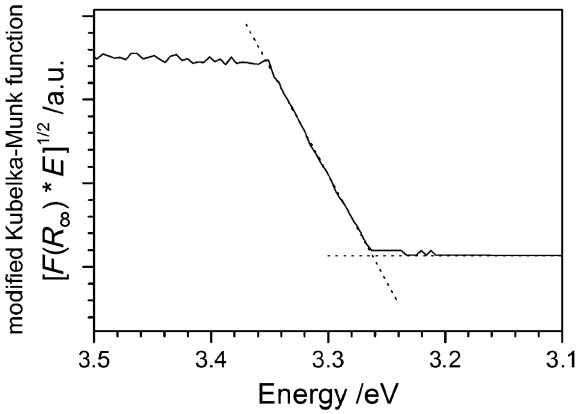

Figure 6. Diffuse-reflectance spectrum of $Cs_2Ga_2S_5$. The bandgap was determined by extrapolation of the linear part of the modified Kubelka–Munk function[33] onto the baseline, as indicated by the dashed lines.

structure, that is, the S33 position was omitted in the first calculations. Structure optimizations with DFT methods resulted in good agreement with experimental interatomic distances. The different Ga–S distances are well reproduced (see Table S3 in the Supporting Information). Lattice parameters are overestimated ($V=547.2$ Å^3, $a=12.710$, $b=7.164$, $c=12.752$, $\beta=109.5^\circ$), which can be attributed to the GGA approach. However, a second reason was found in test calculations assuming full occupation of the S33 position instead of the S3 position. Now, a smaller cell volume and shorter lattice parameters ($V=513.0$ Å^3; $a=12.690$, $b=7.156$, $c=12.127$ Å; $\beta=111.3^\circ$) were predicted, while the overall cell geometry did not change significantly (see also Supporting Information). The result supports the experimentally found possibility of partial substitution of S_2^{2-} entities by S^{2-}. The occupation of the S33 site also has an effect on the calculated bandgap, which increases from 2.45 to 2.73 eV. Additionally, deviations from the value obtained by absorption measurements are also due to the well-known underestimation of bandgaps by DFT methods.[34]

Differences in the bonding behavior of Cs, Ga, and S atoms in the title compound were revealed by atomic sites and orbital projected density of states (PDOS, Figure 7a). Cs shows a typical ionic character with unoccupied 6s states. In contrast, at least partially covalent bonds are derived from the splitting of Ga 4s and 4p orbitals into occupied bonding and unoccupied antibonding DOS contributions. The DOS also reveals the different bonding situations for the S atoms. For all S sites the occupied S 3s states below −13 eV and large 3p contributions below the Fermi energy E_F indicate ionic states S^{2-} and $(S_2)^{2-}$ to a rough approximation. However, partial covalent interactions with hybridized Ga 4s and 4p orbitals must be concluded from DOS maxima below and above E_F. The S3 sites, which form covalent S–S bonds, differ mainly from S1 and S2 sites due to the prominent maxima at −4 and +2 eV, which correspond to the bonding and antibonding σ(p) states. The latter form the LUMO, while the HOMO mainly consists of occupied π(p)* states of the S_2 unit and weak contributions of nonbonding 3p states of S1 and S2 (Figure 7b).

The interpretation of the bonding situation of Cs, Ga, and S atoms is underlined from the integrated orbital occupation (IDOS), which results from covalent and ionic interactions of atomic orbitals (Figure 7c). Therein, the behavior of the Cs 6s orbitals corresponds to unoccupied states above E_F with a corresponding IDOS close to 0e. The contrary is found for S 3s, for which the integration of the occupied states is close to 2e. In both cases, the deviations from integer values are due to weak interactions that cause some occupied bonding and empty antibonding states. The Ga 4s orbitals show a balanced state. Here, the calculated occupation of 1.0e signals that the respective atomic orbital contributes 50% to the occupied and the unoccupied MOs. Finally, the interaction of the Ga 4p and S 3p states is polar, that is, Ga 4p contributes preferably to the antibonding states, whereas S 3p states are the major contributors to the bonding states. A detailed description of the respective DOS and IDOS contributions is provided in the Supporting Information.

In the case of the 3p states that form 3 MOs with neighboring atoms, IDOS = 0 (IDOS = 6e) is expected in the completely cationic (anionic) case and IDOS = 3e in the covalent case. IDOS values for S 3p (4.6e) and Ga 3p (1.4e) indicate a situation between completely ionic and covalent for the Ga–S interactions in $Cs_2Ga_2S_5$. Interestingly, the 3p occupations for the S1, S2, and S3 sites in $Cs_2Ga_2S_5$ do not differ. This is attributed to charge balancing by bonds to Ga.

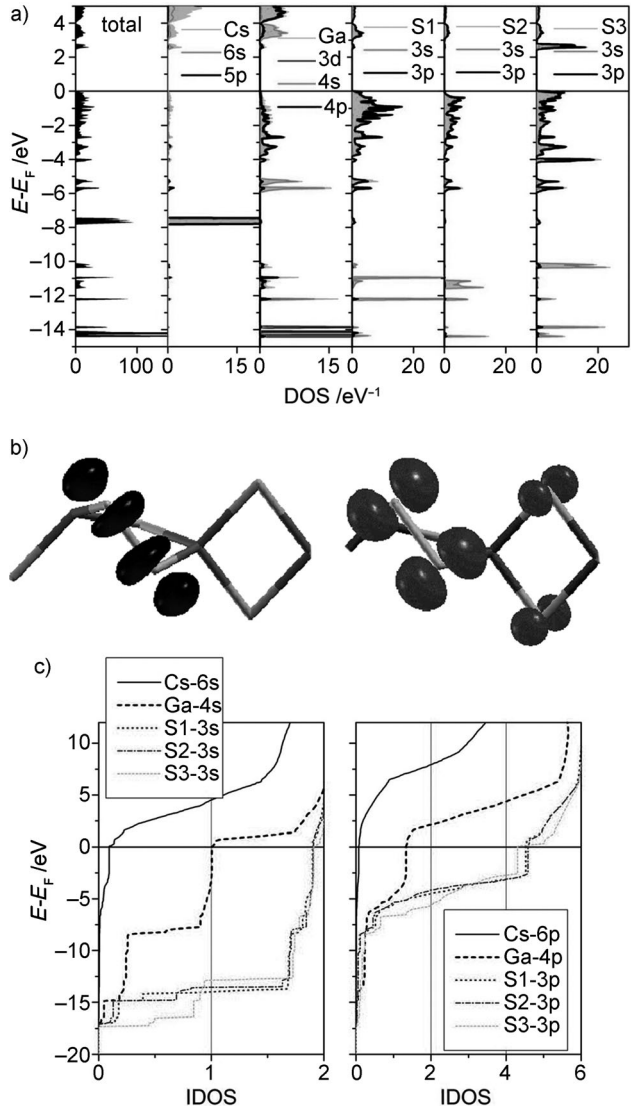

Figure 7. a) Calculated total (TDOS) and partial density of states (PDOS) for $Cs_2Ga_2S_5$ (GGA). b) Visualization of HOMO (grey) and LUMO (black). c) Integrated density of states for valence s and p states of Cs, Ga, and S sites.

Bonding was also analyzed in direct space (see Supporting Information). Charge-difference plots show mainly the additional charge shift to the S atoms within the anionic chains, which is the difference between calculated charge density and the superposition of atomic orbitals. The electron localization function (ELF,[35] Figure 7b) indicates bonding and free electron pairs by maxima with values close to ELF = 1. For the title compound such maxima are found in the center of the S–S bonds. The polarized Ga–S bonds are characterized by respective maxima close to the S atoms. A region of lower ELF around the Ga atoms indicates the contribution of the Ga valence (4s, 4p) orbitals. Atomic charges, as revealed by the Bader[36,37] method of zero-flux surface integration, are +0.9 (Cs), +1.2 (Ga), −0.9 (S1, S2), and −0.6 (S3). They are clearly the result of ionic (Cs), and polarized covalent bonding (Ga, S), respectively.

Conclusion

$Cs_2Ga_2S_5$, a new phase in the ternary systems consisting of alkali metal, gallium, and sulfur, was prepared and structurally characterized. The compound is the first example featuring thiogallate chains $^1_\infty[Ga_2S_3(S_2)^{2-}]$. The compound was further characterized by Raman and UV/Vis spectroscopy. The crystal structure and Raman data are in good agreement with results of DFT calculations. The analysis of the chemical bonding behavior revealed polarized and fully covalent bonds for Ga–S and S–S, whereas Cs forms completely ionic bonds.

Experimental Section

Synthesis

Synthesis of GaS: GaS was synthesized from gallium (Chempur 99.99%) and sulfur (Chempur 99.999%) by chemical vapor transport with iodine (Sigma-Aldrich 99.8%) as transport agent.[38] Passing hydrazoic acid, obtained by acidifying an aqueous solution of NaN_3 (Sigma-Aldrich 99.0%), into an aqueous solution of Cs_2CO_3 (Sigma-Aldrich 99.9%) yielded pure CsN_3. **Caution!** Condensed HN_3 is highly explosive. Tools made from transition metals must be avoided.

Synthesis of $Cs_2Ga_2S_5$: The title compound was synthesized by slow thermal decomposition of CsN_3 mixed with stoichiometric amounts of GaS and S in a quartz glass ampoule under dynamic-vacuum conditions. The formation of $Cs_2Ga_2S_5$ seems to be favored by a cesium polysulfide flux, generated in situ. The raw product was annealed in a flame-sealed ampoule for several days at 803 K in a tube furnace. $Cs_2Ga_2S_5$ does not dissolve in common protic organic solvents. The excess of red Cs_2S_6 formed during the reaction was removed with *N*,*N*-dimethylformamide (Roth 99%) to give a blue, air- and moisture-sensitive solution. Residues of GaS remained in the samples due to polysulfide formation. These yellow plates were manually removed under a microscope.

Crystal growth of Cs_2S_6

Single-crystals of Cs_2S_6 were obtained by solvothermal reaction of stoichiometric amounts of Cs_2CO_3 and S in ethanol (Sigma-Aldrich p.a.) in a sealed quartz-glass ampoule (diameter 1.4 cm, length 10 cm). The ampoule was heated in a stainless steel autoclave at 393 K for several days to yield dark red needles of up to 2 cm length (yield: 85%). Crystals of Cs_2S_6 are sensitive to moist air and decompose within several minutes.

Single-crystal X-ray diffraction

Suitable single-crystals were placed on top of a glass fiber for X-ray diffraction experiments. Data collection was performed on an Agilent Supernova at 123 K or 293 K with monochromatic $Mo_{K\alpha}$ radiation ($\lambda = 0.71073$ Å). Diffraction data were corrected for Lorentzian and polarization effects, and absorption was corrected by an analytical absorption correction implemented in the CrysAlisPro software package.[18] The data sets had a completeness of 99.9% ($Cs_2Ga_2S_5$) and 94.8% (Cs_2S_6) within $2\theta = 50^\circ$. Table 1 summarizes the experimental parameters. The CrysAlisPro software package[18] was used to process the data. The crystal structure was solved by charge-flipping methods with SUPERFLIP[19] (implemented in Jana2006)[20] and refined on F^2 with Jana2006[20] by full-matrix least squares methods. The occupation factors of S3 and S33 were con-

strained during the refinement to take the disorder in the structure into account.

X-ray powder diffraction

X-ray powder diffraction patterns of the title compounds were measured with a STOE STADI P diffractometer equipped with a Dectris Mythen 1 K detector at 293 K. Monochromatized $Cu_{K\alpha1}$ radiation ($\lambda = 1.540598$ Å) was used for $Cs_2Ga_2S_5$ (flat sample), and $Mo_{K\alpha1}$ radiation ($\lambda = 0.70926$ Å) for Cs_2S_6 (capillary). The data were processed by using the WinX^{POW} software package from STOE & Cie.[39]

Vibrational spectroscopy

Vibrational Raman spectra were recorded on a Varian FTS 7000e spectrometer with a Varian FT-Raman unit in the region of 120–4000 cm^{-1} with a resolution of 1 cm^{-1}. The excitation wavelength of 1064 nm was provided by an Nd:YAG laser.

UV/Vis spectroscopy

Diffuse-reflectance measurements were performed with a Bruins Omega 20 UV/Vis spectrometer by using $BaSO_4$ as a reference (100% reflectance). A modified Kubelka–Munk function was used to calculate the absorption data.[33]

Theoretical studies

The CRYSTAL09 code[40] was used for structural optimizations and subsequent calculation of the Raman spectrum. The spectra were fitted, plotted, and visualized with the help of the J-ICE software package.[41] All-electron basis sets were used for all atoms (see applications in ref. [42]), a *k*-mesh sampling of $12\times12\times12$ and 10^{-8} a.u. difference in energy in the last two steps were used to ensure convergence. In this case as well as in the DOS calculations, the GGA functional of Perdew, Burke, and Ernzerhoff (PBE)[43] was applied. Electronic-structure calculations were performed with the full potential local orbital (fplo) method, as implemented in fplo9.00-34.[44] The IDOS analysis was applied as recently described in [45]. Analysis according to the electron localization function (ELF) and the theory of electrons in molecules[36] were performed with Topond.[37,46]

Keywords: cesium · density functional calculations · gallium · solid-state structures · sulfur

[1] B. Krebs, *Angew. Chem. Int. Ed.* **2006**, *45*, 1234; *Angew. Chem.* **2006**, *95*, 113–134.
[2] J.-J. Zondy, F. Bielsa, A. Douillet, L. Hilico, O. Acef, V. Petrov, A. Yelisseyev, L. Isaenko, P. Krinitsin, *Opt. Lett.* **2007**, *32*, 1722–1724.
[3] V. Petrov, A. Yelisseyev, L. Isaenko, S. Lobanov, A. Titov, J.-J. Zondy, *Appl. Phys. B* **2004**, *78*, 543–546.
[4] D. Schmitz, W. Bronger, *Z. Naturforschung B* **1975**, *30*, 491–493.
[5] M. Suseela Devi, K. Vidyasagar, *J. Chem. Soc. Dalton Trans.* **2002**, 4751–4754.
[6] M. Schlosser, V. Frettlöh, H.-J. Deiseroth, *Z. Anorg. Allg. Chem.* **2009**, *635*, 94–98.
[7] D. Friedrich, A. Pfitzner, M. Schlosser, *Z. Anorg. Allg. Chem.* **2012**, *638*, 1572.
[8] D. Friedrich, M. Schlosser, A. Pfitzner, *Z. Anorg. Allg. Chem.* **2014**, *640*, 826–829.
[9] S. J. Ewing, A. Powell, P. Vaqueiro, *J. Solid State Chem.* **2011**, *184*, 1800–1804.
[10] X. Zhand, Z. X. Lei, W. Luo, W. Q. Mu, X. Zhang, Q. Y. Zhu, *Inorg. Chem.* **2011**, *50*, 10872–10877.
[11] W. W. Xiong, J. R. Li, M. L. Feng, X. Y. Huang, *CrystEngComm* **2011**, *13*, 6206–6211.
[12] S. J. Ewing, M. L. Romero, J. Hutchinson, A. V. Powell, P. Vaqueiro, *Z. Anorg. Allg. Chem.* **2012**, *638*, 2526–2531.
[13] H. G. Yao, M. Ji, S. H. Ji, Y. L. An, *Z. Anorg. Allg. Chem.* **2012**, *638*, 683–687.
[14] S. C. Abrahams, E. Grison, *Acta Crystallogr.* **1953**, *6*, 206–213.
[15] A. Hordvik, E. Sletten, *Acta Chem. Scandinavica* **1968**, *22*, 3029–3030.
[16] T. Schleid, P. Lauxmann, C. Graf, C. Bartsch, T. Doert, *Z. Naturforsch.* **2009**, *##64B*, 189–196.
[17] T. Doert, C. Graf, I. G. Vasilyeva, W. Schnelle, *Inorg. Chem.* **2012**, *51*, 282–289.
[18] Agilent Technologies XRD Products, CrysAlisPro, Version 171.36.32, **2013**.
[19] L. Palatinus, G. Chapuis, *J. Appl. Crystallogr.* **2007**, *40*, 786–790.
[20] V. Petricek, M. Dusek, L. Palatinus, *Z. Kristallogr.* **2014**, *229*, 345–352.
[21] J. Do, M. G. Kanatzidis, *Z. Anorg. Allg. Chem.* **2003**, *629*, 621–624.
[22] A. Gutzmann, W. Bensch, *Solid State Sci.* **2002**, *4*, 835–840.
[23] D. P. Shoemaker, C. Y. Chung, J. F. Mitchell, T. H. Bray, L. Soderholm, P. J. Chupas, M. G. Kanatzidis, *J. Am. Chem. Soc.* **2012**, *134*, 9456–9463.
[24] J. Gretzschmann, S. Kaskel, *Z. Anorg. Allg. Chem.* **2014**, *640*, 905–906.
[25] T. J. McCarthy, X. Zhang, M. G. Kanatzidis, *Inorg. Chem.* **1993**, *32*, 2944–2948.
[26] S. L. Nguyen, J. I. Jang, J. B. Ketterson, M. G. Kanatzidis, *Inorg. Chem.* **2010**, *49*, 9098–9100.
[27] H. Sommer, R. Hoppe, *Z. Anorg. Allg. Chem.* **1977**, *429*, 118–130.
[28] P. Böttcher, *J. Less-Common Met.* **1979**, *63*, 99–103.
[29] P. Böttcher, *Z. Anorg. Allg. Chem.* **1980**, *461*, 13–21.
[30] P. Böttcher, K. Kruse, *J. Less-Common Met.* **1982**, *83*, 115–125.
[31] C. Bartsch, T. Doert, *Solid State Sci.* **2012**, *14*, 515–521.
[32] M. J. Taylor, *J. Raman Spectrosc.* **1973**, *1*, 355–358.
[33] H. Kisch, *Angew. Chem. Int. Ed.* **2013**, *52*, 812–847; *Angew. Chem.* **2013**, *125*, 842–879.
[34] R. Dovesi, R. Orlando, A. Erba, C. M. Zicovich-Wilson, B. Civalleri, S. Casassa, L. Maschio, M. Ferrabone, M. De La Pierre, P. D'Arco, Y. Noël, M. Causà, M. Rérat, B. Kirtman, *Int. J. Quantum Chem.* **2014**, *114*, 1287–1317.
[35] D. Becke, K. E. Edgecomb, *J. Chem. Phys.* **1990**, *92*, 5397–5403.
[36] R. F. W. Bader, in *Atoms in Molecules*, Clarendon, Oxford, **1990**.
[37] C. Gatti, V. R. Saunders, D. Roetti, *J. Chem. Phys.* **1994**, *101*, 10686–10696.
[38] G. Micocci, R. Rella, P. Siciliano, A. Tepore, *J. Appl. Phys.* **1990**, *68*, 138–142.
[39] STOE WinX^{POW,} Version 3.06, STOE & Cie GMBH, Darmstadt **2009**.
[40] R. Dovesi, V. R. Saunders, R. Roetti, R. Orlando, C. M. Zicovich Wilson, F. Pascale, B. Civalleri, K. Soll, N. M. Harrison, I. J. Bush, P. D'Arco, M. Llunnell, CRYSTAL09 User's Manual, University of Torino, Torino, **2009**.
[41] P. Canepa, R. M. Hanson, P. Ugliengo, M. Alfredsson, *J. Appl. Crystallogr.* **2011**, *44*, 225–229.
[42] J. Anusca, A. Schmid, P. Peter, J. Rothballer, F. Pielnhofer, R. Weihrich, *Z. Anorg. Allg. Chem.* **2009**, *635*, 2410–2428.
[43] J. P. Perdew, K. Burke, M. Emzerhof, *Phys. Rev. Lett.* **1996**, *77*, 3865–3868.
[44] K. Koepernik, H. Eschrig, *Phys. Rev. B* **1999**, *59*, 1743–1757.
[45] J. Rothballer, F. Bachhuber, F. Pielnhofer, F. M. Schnappacher, R. Pöttgen, R. Weihrich, *Eur. J. Inorg. Chem.* **2013**, *2*, 248–255.
[46] C. Gatti, S. Casassa, TOPOND User's Manual, CNR-ISTM of Milano, Milano, **2014**.

Received: August 19, 2014
Published online on November 21, 2014